Molecular Biology of the Cell
Vol. 12, 3644–3657, November 2001

Novel Stress-responsive Genes EMG1 and NOP14 Encode Conserved, Interacting Proteins Required for 40S Ribosome Biogenesis

Phillip C. C. Liu* and Dennis J. Thiele†

Department of Biological Chemistry, The University of Michigan Medical School, Ann Arbor, Michigan 48109-0606

Submitted May 15, 2001; Revised August 1, 2001; Accepted August 14, 2001
Monitoring Editor: Elizabeth Craig

Under stressful conditions organisms adjust the synthesis, processing, and trafficking of molecules to allow survival from and recovery after stress. In baker's yeast *Saccharomyces cerevisiae*, the cellular production of ribosomes is tightly matched with environmental conditions and nutrient availability through coordinate transcriptional regulation of genes involved in ribosome biogenesis. On the basis of stress-responsive gene expression and functional studies, we have identified a novel, evolutionarily conserved gene, *EMG1,* that has similar stress-responsive gene expression patterns as ribosomal protein genes and is required for the biogenesis of the 40S ribosomal subunit. The Emg1 protein is distributed throughout the cell; however, its nuclear localization depends on physical interaction with a newly characterized nucleolar protein, Nop14. Yeast depleted of Nop14 or harboring a temperature-sensitive allele of *emg1* have selectively reduced levels of the 20S pre-rRNA and mature18S rRNA and diminished cellular levels of the 40S ribosomal subunit. Neither Emg1 nor Nop14 contain any characterized functional motifs; however, isolation and functional analyses of mammalian orthologues of Emg1 and Nop14 suggest that these proteins are functionally conserved among eukaryotes. We conclude that Emg1 and Nop14 are novel proteins whose interaction is required for the maturation of the 18S rRNA and for 40S ribosome production.

INTRODUCTION

Under stressful conditions, organisms adjust the synthesis, processing, and trafficking of molecules to allow survival from and recovery after stress. Because production of ribosomes is one the cell's most energy-demanding processes, regulation of ribosomal biogenesis is tightly coordinated with environmental growth conditions. In the baker's yeast *Saccharomyces cerevisiae*, this regulation occurs primarily at the level of transcription of genes encoding ribosomal proteins (RPs) and other factors engaged in processing and assembly of these particles (Planta, 1997; Warner, 1999). Many factors involved in this pathway have been identified by isolating genetic mutants that fail to process the pre-rRNA into its mature components. With the complete sequence of the yeast genome, additional factors have been identified by searching for sequences in the database with strong homology to characterized proteins involved in this process (Kressler *et al.*, 1997); however, this approach is limited to proteins with well-defined biochemical functions or functional motifs. Genomic and proteomic approaches based on strategies designed to characterize all components of functional or interacting protein complexes, such as the nuclear pore complex (Rout *et al.*, 2000), or systematic localization of yeast proteins (Ross-Macdonald *et al.*, 1999) are likely to identify novel candidate factors involved in ribosome biogenesis and trafficking.

Another powerful strategy for identifying proteins that are functionally related is to characterize genes that are transcriptionally linked. Proteins involved in the same biochemical process or regulatory circuit are frequently coregulated under specific growth conditions. Genome-wide analyses of mRNA expression data under conditions of cellular stress, nutrient deprivation, or cell differentiation have revealed large groups of such coregulated genes (DeRisi *et al.*, 1997; Holstege *et al.*, 1998; Chu *et al.*, 1998; Gasch *et al.*, 2000; Causton *et al.*, 2001). The expression of RP genes is tightly coordinated with changes in nutrient status and environmental stress (Planta, 1997). For example, during heat shock, the levels of mRNAs encoding RPs and other factors involved in ribosome biogenesis are transiently decreased (Gorenstein and Warner, 1976; Kim and Warner, 1983; Herruer *et al.*, 1988; Eisen *et al.*, 1998). Analysis of the promoter sequences of RP genes has led to the identification of con-

* Present address: Applied Biotechnology, Dupont Pharmaceuticals Co., P.O. Box 80, Bldg. 336, Wilmington, DE 19880-0361.
† Corresponding author. E-mail address: dthiele@umich.edu.

Table 1. Yeast strains used in this study

Strain	Genotype	Source
W303-1a	*MAT***a** *ade2-1 leu2-3,112 ura3-1 his3-11,15 trp1-1 can1-100*	
W303-1α	*MATα ade2-1 leu2-3,112 ura3-1 his3-11,15 trp1-1 can1-100*	
W303-a/α	Diploid strain created by mating W303a and W303a	This study
PLY12	W303-1α, *emg1*::*LEU2* (p416A*DH-EMG1*)	This study
PLY12 (EMG1)	PLY12 (pRS414-*EMG1*)	This study
PLY12 (HA-EMG1)	PLY12 (pRS414-*HA(3)-EMG1*)	This study
PLY12 (MYC-EMG1)	PLY12 (pRS414-*MYC(3)-EMG1*)	This study
PLY12 (*emg1-1*)	PLY12 (pRS414-*emg1-1*)	This study
PLY12 (*MYC-emg1-1*)	PLY12 (pRS414-*MYC(3)-emg1-1*)	This study
PLY13	W303-1a, *emg1*::*LEU2* (p416A*DH-EMG1*)	This study
PLY20	W303-1α, *emg1*::*LEU2 his3*::*HIS3*::*MYC(2)-EMG1*	This study
PLY21	W303-1α, *emg1*::*LEU2 his3*::*HIS3*::*MYC(2)-emg1-1*	This study
PLY22	W303-1α, *Nop14*::*KAN*^{R} p426*GPD-NOP14*	This study
PLY23	W303-1a, *Nop14*::*KAN*^{R} p426*GPD-NOP14*	This study
PLY23 (NOP14)	PLY23 (pRS413-*NOP14*)	This study
PLY23 (GAL-NOP14)	PLY23 (YCp*GAL1*::*NOP14-FLAG(2)*)	This study
PLY23 (NOP14-FLAG)	PLY23 (pRS413-*NOP14-FLAG(2)*)	This study
PLY23 (NOP14-GFP)	PLY23 (pRS413-*NOP14-GFP*)	This study

served *cis*-acting elements that are required for both transcriptional activation and repression. Most RP genes have tandemly arranged binding sites for the essential yeast DNA-binding protein, Rap1, whereas a subset of RP gene promoters harbor sites for another DNA-binding protein, Abf1 (Mager and Planta, 1990; Lascaris *et al.*, 1999). Rap1 was recently shown to both activate and repress transcription from the same *cis*-acting element in the *RPL30* promoter (Li *et al.*, 2000). Intriguingly, an activator of inducible stress response genes, the heat shock transcription factor (HSF1), has also been shown to be involved in the repression of the *SSB1* gene, encoding a ribosome-associated member of the heat shock protein 70 family, and several RP genes after shifts to elevated temperatures. In cells bearing a mutant allele of *HSF1*, the down-regulation of several RP genes was impaired, suggesting that proper sensing of thermal stress by Hsf1 was necessary for the specific and coordinate repression of RP genes (Lopez *et al.*, 1999).

The assembly of the ribosome occurs in the nucleolus, a specialized, electron-dense region of the nucleus (Scheer and Hock, 1999). In eukaryotes, three of the rRNAs components of the ribosome are transcribed by RNA polymerase I as a precursor rRNA (the 35S RNA in *S. cerevisiae*). One consequence of this coordinate gene regulation is the ability of the cell to produce nearly equimolar amounts of each of the 78 RPs and to match this production with synthesis of rRNA (Warner, 1999). This pre-rRNA is assembled with RPs to form a 90S preribosomal particle. Through a series of post-transcriptional events including methylation, pseudouridinylation, and processing by endo- and exonucleases, the 35S pre-rRNA is processed into the mature 18S, 5.8S, and 25S rRNAs that are components of the 40S and 60S ribosomal subunits, respectively. Specific factors required for the maturation of the 40S subunit include a number of small nucleolar RNAs (snoRNAs), nucleolar proteins associating with these snoRNAs, RNA helicases, and RNA methylases. Loss-of-function mutants or genetic depletion of these proteins or RNAs leads to a similar terminal phenotype, including the accumulation of the 35S pre-rRNA, decreases in mature 18S rRNA, and a 60S to 40S ribosome subunit imbalance (reviewed by Kressler *et al.*, 1999; and Venema and Tollervey, 1999).

In this paper, we describe the characterization of an essential yeast gene denoted *EMG1* (essential for mitotic growth). The *EMG1* mRNA is strongly repressed during heat shock, like that of RP genes, and encodes an evolutionarily conserved protein involved in the biogenesis of the 40S ribosomal subunit. Emg1 physically interacts with an essential nucleolar protein Nop14 that functions in the same genetic and biochemical pathway as Emg1. The orthologous *EMG1* gene *mraI* from fission yeast was previously isolated as a dosage suppressor of a *ras1* effector domain mutant (Hakuno *et al.*, 1996); however, the function of Mra1 was not elucidated. Here we provide evidence that Emg1 and its interacting partner protein Nop14 are required for appropriate processing of the pre-18S rRNA and small ribosomal subunit assembly.

MATERIALS AND METHODS

Strains

All yeast strains used in the study are listed in Table 1. Yeast cells were grown in standard YPD (1% yeast extract, 2% peptone, 2% glucose) or YPGal (2% galactose) unless otherwise indicated. Strains for which plasmid selection was required were grown in synthetic complete (SC) medium lacking specific nutrients required for selection. DNA was transformed into yeast by the lithium acetate method (Gietz *et al.*, 1992).

Construction of Deletion Strains

A 1.7-kb clone containing the complete *EMG1* open reading frame (ORF) (*YLR186w*) and flanking sequences, from 548 nucleotides (nt) upstream of the ATG to 380 nt downstream of the stop codon, was amplified with the use of high-fidelity polymerase chain reaction (PCR; TaqPlus Turbo, Stratagene, La Jolla, CA) and cloned into pSK to generate pSK−*YLR186*. This plasmid was cut with *Eco*RV and *Sal*I, and the latter site was filled in with Klenow. This digestion results in a gap in the *EMG1* ORF from nt −31 (relative to the ATG)

to nt 661. A blunt-ended fragment containing the *LEU2* gene was ligated to this plasmid, yielding pSK−*ylr186::LEU2*. An *Hin*dIII-XbaI fragment was used to transform W303a/α-diploid cells, and LEU^+ cells were isolated. Correct integration and disruption of the *EMG1* locus was confirmed by Southern blotting. Heterozygous diploids were sporulated in potassium acetate, and the tetrads were dissected by micromanipulation. Strains PLY12 and PLY13 corresponding to *emg1* deletion strains of mating types α and a, respectively, and harboring plasmid p416ADH*EMG1* were derived by this procedure. Plasmid shuffling was performed as previously described with the use of 5-fluoroorotic acid (5-FOA) (Boeke *et al.*, 1987) for selection to create PLY12 or PLY13 derivatives which carry CEN plasmids bearing wild-type or epitope-tagged alleles of *EMG1* (see Table 1 for a complete list of strains) expressed from the endogenous promoter (from nt −548 relative to the ATG). The *NOP14* gene (*YDL148c*) was disrupted in W303 diploids by direct transformation of a linear PCR product composed of the KAN^R gene with 50 bp of flanking sequences corresponding to sequences directly upstream of the *NOP14* ATG and downstream of the translation stop codon (Wach *et al.*, 1994). Transformants were selected on YPD with 400 μg/ml G418. Strains PLY22 and PLY23 corresponding to *Nop14::*KAN^R haploid cells of MATα and MATa were derived by sporulating heterozygous diploids and selecting for KAN^R, URA^+ (p416*GPD-NOP14*) spores. *Nop14* deletion strains bearing CEN plasmids with epitope-tagged alleles of Nop14 expressed from the endogenous promoter were created by plasmid shuffling.

Construction of Epitope-tagged Alleles of EMG1 and NOP14

To generate epitope-tagged alleles of *EMG1*, a *Not*I site was engineered between sequences encoding amino acids Val2 and Glu3 by PCR. The resulting clone *Not*I-*EMG1* has the amino acid sequence MVGGRED at its amino terminus. A pair of complementary oligonucleotides harboring two tandem copies of the MYC epitope (EQKLISEEDL) or three repeats of the hemagluttin (HA) epitope flanked by overhanging *Eag*I sites were synthesized, annealed, and inserted into the *Not*I linearized vector containing *Not*I-*EMG1* to generate plasmids pRS414MYC2-*EMG1* and pRS414HA3-*EMG1*, respectively. To create carboxyl-terminal fusions of Nop14 with the FLAG epitope or green fluorescent protein (GFP), PCR was used to replace the stop codon with an *Not*I site followed by a new termination codon. Complementary *Eag*I flanked oligonucleotides bearing two copies of the FLAG epitope (DYKDDDDK) or an *Not*I linearized fragment of GFP was cloned into the *Not*I-digested vector to generate p413*NOP14-FLAG2* or p413*NOP14-GFP*, respectively. All epitope-tagged alleles of *EMG1* and *NOP14* used in this study were capable of complementing the viability defects of the respective knockout strains when expressed from a CEN plasmid.

Cloning of a cDNA Encoding Mouse Emg1 and Complementation of emg1 Yeast

The sequence encoding the mouse Emg1 (mEMG1) ORF previously described as locus C2F (Ansari-Lari *et al.*, 1998) was cloned by PCR amplification with the use of mouse liver cDNA (gift from Kathryn Tullis) and confirmed by DNA sequencing. The complete mEMG1 ORF was subcloned into p424GPD and transformed into PLY12. The ability of mEmg1 to complement the viability defect of *emg1* yeast was assessed by streaking transformants onto 5-FOA–containing plates to force the loss of the CEN-URA3 plasmid harboring yeast *EMG1*.

Generation of Conditional Alleles of EMG1 and NOP14

A temperature-sensitive allele of *EMG1* was created based on the observation that a point mutation in the conserved central region of the *Schizosaccharomyces pombe mra1* (K213E) led to a protein of altered function (Hakuno *et al.*, 1996). An oligonucleotide (5′-ATAGACCTGGACCN(C,G,T) TCCGGCTTTGTTGATTGG-3′) in which the first two positions of the homologous amino acid (K109) in baker's yeast *EMG1* were randomized and a primer corresponding to the promoter of *EMG1*, we amplified the 5′-end of the *EMG1* gene with the use of error-prone PCR. The product was subcloned into pRS414*EMG1* and transformed into PLY12, and conditional alleles were identified by replica plating the transformants onto 5-FOA-containing plates and incubation of duplicate plates at 23 and 37°C. To generate a conditional allele of *NOP14*, we cloned the *NOP14* ORF into vector YCpGAL1, a CEN, LEU2 plasmid harboring the galactose-inducible, glucose-repressible *GAL1* promoter.

Two-Hybrid Screen and Human Nop14 Cloning

A two-hybrid screen for Emg1-interacting proteins was performed in yeast strain L40 transformed with pLexA-*Emg1* harboring the complete Emg1 protein fused to the LexA DNA-binding domain as bait and the Gal4 activation domain (pGAD)-yeast genomic libraries YL2H-C1, C2, and C3 (gift from Philip James and Elizabeth Craig, University of Wisconsin). From $\sim 10^7$ primary transformants, four different clones survived two rounds of selection after standard protocols (Vojtek *et al.*, 1993). Among these positive clones, only one unique insert corresponded to a predicted ORF YDL148c, which we designate Nop14. To map sites of interaction between Emg1 and Nop14, fragments of the *NOP14* ORF were amplified by PCR, cloned into pGAD, and tested by two-hybrid analysis for interactions. A sequence encoding human Nop14 was cloned by PCR from a cDNA library prepared from Jurkat cells; the amplified sequence is identical to the translated amino acid sequence for gene locus BAA19121 in the human genome database except for one variation, Q732R (Hadano *et al.*, 1998). At this time, it is unclear whether the g to a nucleotide transition is a PCR-generated artifact or a polymorphism. The complete mEMG1 ORF was cloned into pLexA and a fragment of the HsNop14 (amino acids 17–470) was cloned into pVP16-AD and cotransformed into L40 for two-hybrid analysis.

Immunoprecipitation and Immunoblotting

Whole cell extracts were prepared from strain PLY12 harboring plasmids for *HA-EMG1* and *NOP14-FLAG* expressed from their cognate promoters with the use of glass beads and $HEGN_{100}$ buffer (20 mM HEPES, pH 7.9, 1 mM EDTA, 10% glycerol, 100 mM NaCl) as described previously (Liu *et al.*, 1997). Lysates were adjusted to 1% Triton X-100, incubated on ice for 12 min, and then clarified by centrifugation at 200 × *g* for 3 min at 4°C. To ~750 μg of total protein, 15 μl of 50% (vol/vol) M2 anti-FLAG Affigel or 2.5 μg of anti-HA (Berkeley Antibody, Richmond, CA) antibody was added, and lysates were incubated at 4°C on a rotating wheel for 2 h. For extracts receiving the anti-HA primary antibody, protein A/G-Sepharose was also added for the final 1 h of incubation. Immunoprecipitated complexes were washed three times with lysis buffer containing 0.5% Triton X-100, resuspended in 2× SDS loading buffer, heated to 65°C, and loaded onto a 4–15% SDS-polyacrylamide gel. Immunoblotting was performed with anti-MYC, clone 9E10 (Roche, Gipf-Oberfrick, Switzerland), anti-HA, clone 12CA5 (Berkeley Antibody), or anti-FLAG M2 (Sigma, St. Louis, MO), horseradish peroxidase-conjugated secondary antibodies (Amersham, Arlington Heights, IL) and developed with enhanced chemiluminescent detection reagents.

Biochemical Fractionation

Approximately 50 OD_{600} units of strain PLY12 (HA-EMG1) harboring plasmid p413*TEF-NOP14-FLAG* were harvested from midlog cultures and spheroplasted as described by Franzusoff *et al.* (1991). Spheroplasts were resuspended in 1 ml of $HEGN_{100}$ buffer supplemented with a cocktail of protease inhibitors (Roche) and lysed by

two rounds of freezing in a dry ice-ethanol bath and rapid thawing at 30°C. Lysates were centrifuged at 200 × *g* for 2 min at 4°C. In preliminary experiments, this supernatant (total cell extract, T) was centrifuged at 16,000 × *g* for 15 min at 4°C to separate the supernatant (S)16 and pellet (P)16 fractions. The P16 was incubated with 1% Triton X-100 for 30 min on ice and subjected to ultracentrifugation at 100,000 × *g* for 30 min to separate the S100 and P100 fractions. In later experiments, whole cell extracts were divided into four equal aliquots and treated as follows: lysis buffer alone (control) or supplemented with 1 M NaCl, 0.2 M Na_2CO_3 (pH 11), 1% Triton X-100 for 30 min on ice before dilution with an equal volume of $HEGN_{100}$ buffer and centrifuged at 100,000 × *g* for 30 min. The S100 fractions were precipitated with 10% trichloroacetic acid, washed twice with acetone, and resuspended in 2× SDS loading buffer. Samples were analyzed by SDS-PAGE and immunoblotting as described above. Crude nuclei were isolated according to previously described methods (Wise, 1991). The postnuclear fraction was further centrifuged at 100,000 × *g* in a TLS55 rotor (Beckman, Fullerton, CA) for 30 min to yield the cytosolic fraction. Aliquots corresponding to equivalent protein amounts of the original cell extract from the total, postnuclear, and cytosolic fractions were precipitated with trichloroacetic acid as described above before separation on SDS-PAGE.

Microscopic Analysis of Emg1 and Nop14 Localization

Indirect immunofluorescence microscopy was used to localize a MYC2-Emg1 protein. PLY12 (MYC-EMG1) cells were grown in SC-trp medium until midlog phase ($A_{600} < 0.5$) and fixed with 3.7% formaldehyde for 30 min at 23°C. Sphereoplasts were prepared and adhered to poly-lysine–coated multiwell slides. After a 5-min block with TBS (10 mM Tris-HCl, pH 7.4; 150 mM NaCl; 1% bovine serum albumin, cells were incubated with a 1 μg/ml dilution of anti-MYC antibody (Roche) in TBS for 2 h in a humidified chamber. The wells were washed extensively with TBS and then incubated with a 1:1000 dilution of anti-mouse Texas-Red conjugate in TBS (Molecular Probes, Eugene, OR) for another 1 h. After the wells were washed six times with TBS, 1 drop of ProLong mounting medium (Molecular Probes) containing 0.5 μg/ml 4′,6-diamidino-2-phenylindole (DAPI) was added and cells were observed with an Eclipse E800 automated fluorescent microscope (Nikon, Melville, NY) equipped with a digital camera. Images were captured with the use of the ISEE software package (Inovision). Direct fluorescence microscopy was used to detect Nop14-GFP in live cells (PLY23 [NOP14-GFP]) mounted in 1% low-melt agarose. Briefly, cells were grown to midlog phase, harvested, washed, and resuspended in fresh buffered medium (pH 6.5) containing 5 μg/ml Hoechst 33542 stain for 5 min, washed with medium, mixed with melted agarose, and mounted onto glass slides. Images were captured and analyzed as described above. Monoclonal anti-Nop1 antibody mAb A66 was a gift from Dr. John Aris (University of Florida) and used as described previously (Aris and Blobel, 1988).

RNA Isolation and Analysis

Total RNA was isolated from yeast with the use of a modified hot phenol method (Gasch *et al.*, 2000), and Northern hybridization was carried out using standard protocols with end-labeled oligonucleotide probes (ordered according to Figure 6A): (a, 5′ETS) 5′-CCAGATAACTATCTTAAAAG; (b, 18S) 5′-CATGGCTTAATCTTTGAGGAC; (c, ITS1–5′) 5′-CGGGTTTTAATTGTCCTA; (d, ITS1–3′) 5′-CCAGTTACGAAAATTCTG; (e, 25S) 5′-TACTAAGGCAATCCGGTTGG. Pulse-chase labeling of cells was performed essentially as described with L-[*methyl*-^{3}H]methionine (Kressler *et al.*, 1997). For characterization of the *emg1-1* mutant, strain PLY21 and isogenic wild-type controls (W303–1a) were grown until midlog phase at the permissive temperature of 23°C, diluted into warmed (37°C) YPD to an A_{600} of 0.05 and cultured for 10 h at the restrictive temperature of 37°C. For analysis of the PLY23 (*GAL-NOP14)* strain, cells were grown in YPGal (2%) Raf (2%) until midlog phase, washed, and then diluted into fresh YPGal/Raf or YPD and incubated for 9 h. Approximately 20,000 cpm of each RNA sample was resolved on a 1.2% agarose 0.67 M fomaldehyde/3-(*N*-morpholino)propanesulfonic acid gel. After transfer to a nylon filter, the membrane was soaked in Autofluor (National Diagnostics, Atlanta, GA) and exposed to x-ray film with an intensifying screen for 4 d.

Polysome Analysis

Polysomes were prepared from yeast cells as described by Baim *et al.* (1985) with minor changes. Cultures were grown to a density between A_{600} 0.5 and 0.9 under the appropriate conditions to manifest mutant phenotypes as described above. Before harvesting cells, cycloheximide was added to a final concentration of 0.05 mg/ml. Extracts were prepared by glass bead lysis of cell pellets in 10 mM Tris-HCl (pH 7.5), 100 mM NaCl, 30 mM $MgCl_2$, 0.05 mg/ml cycloheximide, and 0.2 mg/ml heparin. Approximately 10 A_{260} units of extract were layered over a 10.5-ml 7–47% sucrose gradient and centrifuged in a Beckman SW41 rotor at 39,000 rpm at 4°C for 2.75 h. The gradients were analyzed with a continuous gradient collector with the UV detector set to 254 nm. To dissociate ribosomes into subunits, cell cultures were treated with 0.1 mg/ml NaN_3 for 20 min before harvesting and then lysed in 10 mM Tris-HCl (pH 7.5), 50 mM NaCl buffer, and centrifuged over a 7–47% sucrose gradient prepared with the same buffer and analyzed as above.

RESULTS

A Novel Stress-responsive mRNA Encodes an Essential, Conserved Protein Emg1

We identified *EMG1* as a novel stress-responsive gene whose expression is strongly, but transiently, repressed during heat shock (Figure 1A). Levels of the *EMG1* mRNA were similarly reduced during other stress conditions, including oxidative and osmotic shock, and during stationary phase (data not shown). In contrast, a classical heat shock protein gene, *SSA1,* is strongly and transiently induced during these treatments. Many mRNAs encoding growth regulatory proteins including RPs, such as *RPL18* and *RPS19*, show transient decreases during stress with similar kinetics and magnitude as the *EMG1* mRNA (Figure 1A). Indeed, cluster analysis of gene expression patterns from data generated from a DNA microarray experiment with the use of RNA isolated from yeast exposed to a variety of physiological and environmental stresses revealed that *EMG1* expression patterns were most similar to a number of genes encoding factors involved in rRNA transcription and processing and RPs (Gasch *et al.*, 2000). The Emg1 protein sequence is highly conserved among eukaryotes with greatest homology in the central region (Figure 1B). The *S. pombe* orthologue of *EMG1* (Mra1) was previously recovered as a dosage suppressor of an effector domain mutant of *ras1* (T40S) that led to inefficient mating (Hakuno *et al.*, 1996). Disruption of the *EMG1* gene revealed that it is essential in baker's yeast as is the *mra1* gene in *S. pombe* (Figure 1C). A gene dosage screen with the use of a 2μ yeast genomic library to suppress the lethal phenotype of *emg1*Δ cells recovered only *EMG1* (>40 times), suggesting that the Emg1 protein has an essential nonredundant cellular function. Molecular cloning and expression of the mouse orthologue of *EMG1* in yeast demonstrates that *mEMG1* is capable of suppressing the viability defect of *emg1* cells and indicates that Emg1 is both struc-

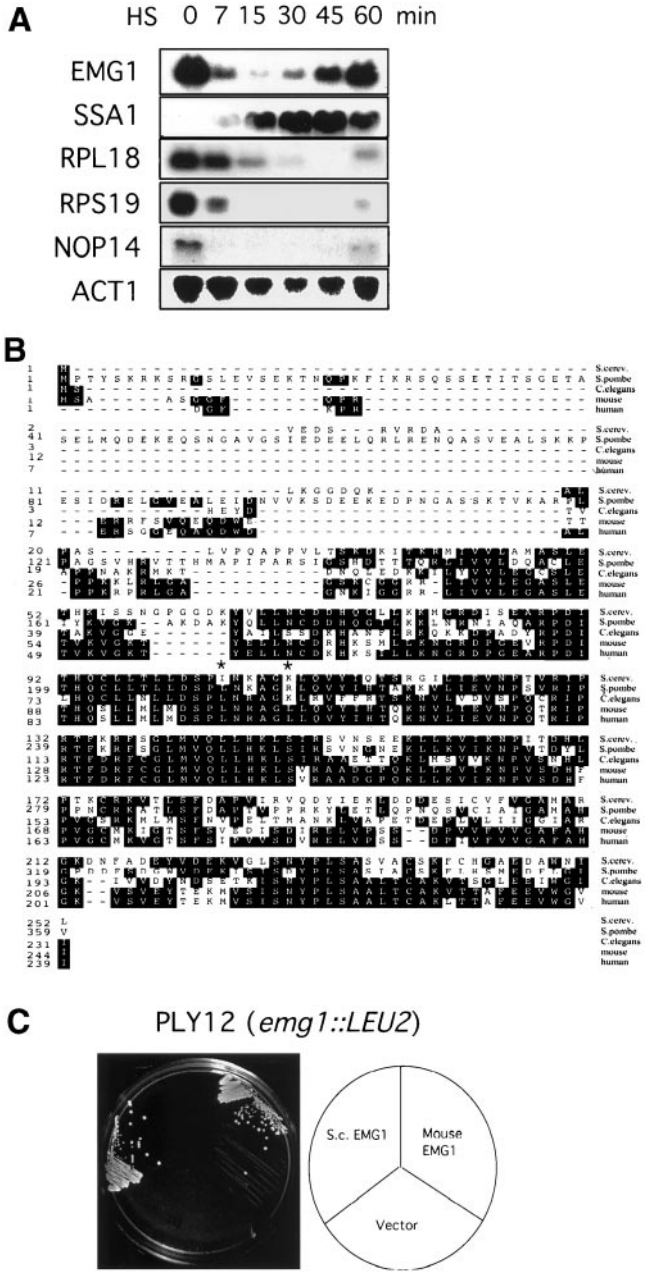

Figure 1. The stress-responsive gene *EMG1* encodes an essential, conserved protein. (A) Northern blot analysis of Emg1 mRNA in response to thermal stress. Total RNA was isolated over the indicated time course from W303–1α cells exposed to a heat shock temperature of 39°C and probed with DNA fragments specific to *EMG1*, the Hsp70 gene *SSA1*, RP genes *RPL18* and *RPS19*, *NOP14*, or actin (*ACT1*). (B) Alignment of the amino acid sequences for Emg1 (*YLR186w*), the *S. pombe Mra1*, and worm, mouse, and human orthologues. The asterisks denote amino acids that are mutated the temperature-sensitive allele *emg1-1*. (C) Mouse *EMG1* complements the viability defect of *emg1* yeast. PLY12 (*emg1:: LEU2*, p416ADH-*EMG1*) cells were transformed with plasmids pRS414 (vector), pRS414*EMG1*, or p414GPD-m*EMG1*, and transformants were streaked onto 5-FOA-containing plates and incubated for 3 d at 30°C. S.c., *S. cerevisiae*.

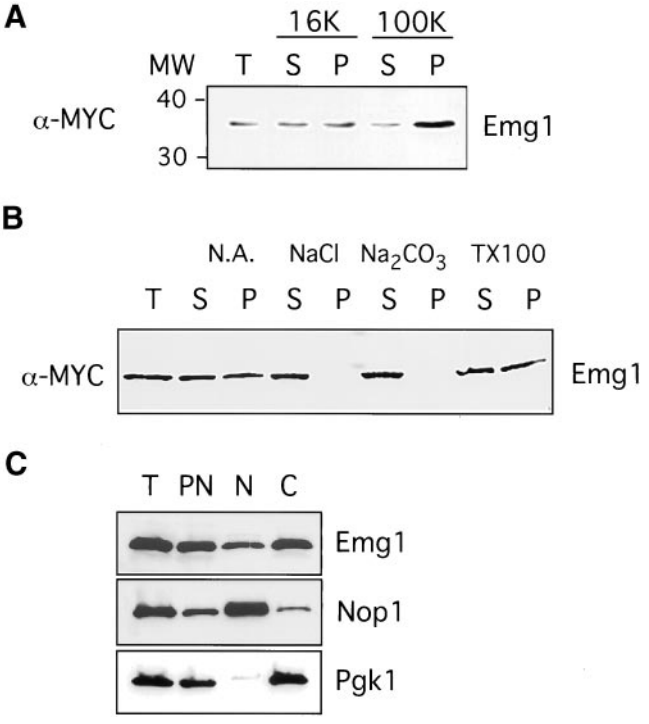

Figure 2. Biochemical fractionation of Emg1. (A) Emg1 fractionates into both soluble and sedimentable fractions. Extracts prepared from PLY12 (MYC-EMG1) cells were fractionated as described in MATERIALS AND METHODS and analyzed by SDS-PAGE and immunoblotting with anti-MYC antibody. Equivalent amounts of the total lysate (T) and supernatant (S) or pellet (P) fractions from each centrifugation were loaded. (B) Equal amounts of total cell lysates were left untreated (N.A.) or adjusted to 1 M NaCl, 0.2 M Na_2CO_3 (pH 11), or 1% Triton X-100 (TX100) and centrifuged at 100,000 $\times$ *g* for 30 min before analysis by immunoblotting with anti-MYC antibody. (C) Emg1 is localized to both nuclear and cytosolic fractions. Yeast nuclei (N) and cytosol (C) were prepared from total cell lysates (T) of PLY12 (HA-EMG1) as described. PN refers to the crude postnuclear fraction. Immunoblotting was performed for HA-Emg1, the nuclear protein Nop1, and Pgk1 with the use of specific antibodies.

turally and functionally conserved among these eukaryotes (Figure 1C).

Analysis of the Emg1 amino acid sequence with the use of a number of computer algorithms did not reveal any characteristic motifs that would suggest a function for this protein. Therefore, to characterize Emg1 further, we first performed biochemical fractionation experiments to determine its localization. Approximately half of the cellular Emg1 was found in the soluble fraction after a low (16,000 $\times$ *g*) centrifugation and half was found in the pellets (Figure 2A). On solubilization of the pellet and ultracentrifugation at 100,000 $\times$ *g*, Emg1 was again found in both soluble and pellet fractions, suggesting that Emg1 is widely distributed and may interact with potential membrane components or aggregates. To ascertain the nature of the interaction between Emg1 and the membrane fractions, we treated the low-speed pellets with NaCl, Na_2CO_3, or Triton X-100 and separated the soluble proteins from the pellets by ultracen-

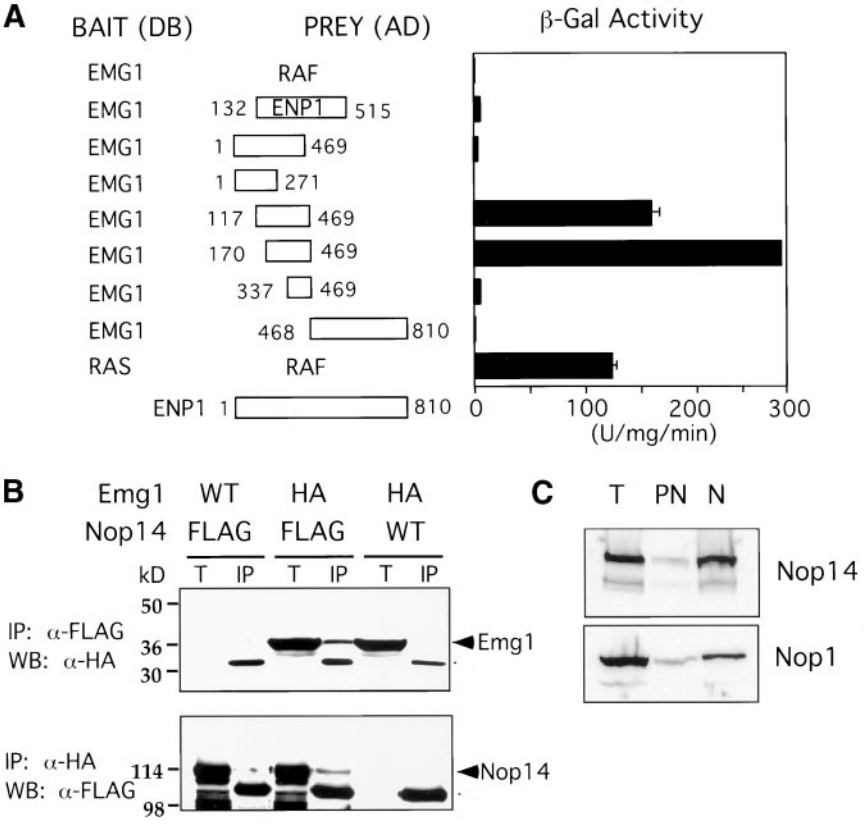

Figure 3. Emg1 interacts specifically with the Nop14 protein. (A) Mapping the region of Nop14 that interacts with Emg1 by two-hybrid analysis. A p*LexA*DB-*EMG1* fusion was coexpressed with a series of pGAD-*NOP14* truncations in the L40 strain. Positive interactions between the proteins was detected by liquid β-galactosidase assays. Human Ras and Raf proteins served as controls for the assay. The *NOP14* ORF encodes an 810-amino acid protein. (B) Coimmunoprecipitation experiments confirm an interaction between Emg1 and Nop14 in vivo. Extracts prepared from PLY12 (EMG1) or PLY12 (HA-EMG1) transformed with p413TEF-*NOP14*-FLAG2 or wild-type (WT) *NOP14* were subjected to immunoprecipitation (IP) with anti-FLAG (M2) Affigel or anti-HA (12CA5) antibody and detected by immunoblot analysis with the use of the reciprocal antibody. The black arrowheads indicate HA-Emg1 (top) or Nop14-FLAG (bottom) and the white arrowheads show positions of the immunoglobulin chains. (C) Nop14 is a nuclear protein. Equivalent aliquots of total cell extracts (T) and crude nuclear (N) and postnuclear (PN) fractions were prepared from PLY23 (Nop14-FLAG) and analyzed for the distribution of Nop14 or Nop1 by immunoblotting with the use of anti-HA and anti-Nop1 antibodies, respectively.

trifugation. As shown in Figure 2B, Emg1 was efficiently liberated to the supernatant by treatment with NaCl or Na_2CO_3, suggesting that Emg1 associates through electrostatic interactions with itself or other proteins found in the high-speed pellet. To determine the intracellular localization of Emg1, we fractionated cells into crude nuclear, postnuclear, and cytosolic fractions. HA-Emg1 was detected in both the nuclear and cytosolic fractions. The nuclear protein fibrillarin (Nop1) was detected predominantly in the nuclear fraction with only a trace in the cytosol, perhaps representing newly synthesized protein or contamination due to leakage from the nucleus during extract preparation. In contrast, the cytosolic enzyme phosphoglycerate kinase (Pgk1) was almost exclusively found in the cytosolic fraction, indicating minimal contamination of the nuclei by soluble proteins. Together, these data suggest that Emg1 is found in both the nucleus and the cytosol and that a pool of Emg1 is associated with a membrane fraction.

Emg1 Physically Interacts with the Essential Protein Nop14

To identify the interacting partner protein(s), we carried out a two-hybrid screen with the use of the full-length *EMG1* ORF fused to the *LexA* DNA-binding domain as bait and a genomic yeast library fused to the Gal4 activation domain. From $>10^7$ primary transformants, only one unique sequence was isolated that mapped to a predicted ORF. This sequence corresponded to amino acids 132–515 of the uncharacterized yeast ORF *YDL148c,* henceforth designated *NOP14* (nucleolar protein 14). Deletion mapping revealed that the central domain of Nop14 from amino acids 170–469 is sufficient for interaction between Emg1 and Nop14 by two-hybrid analysis. The amino-terminal region of Nop14 (construct aa 1–271) failed to interact with Emg1, whereas removal of the first 117 amino acids significantly enhanced this interaction (compare constructs aa 1–469 vs. 117–469). *NOP14* is an essential gene in yeast (data not shown), and like *EMG1*, *NOP14* mRNA levels are abundant during nutrient-replete growth conditions but are rapidly and transiently repressed during heat shock (Figure 1A). Furthermore, *NOP14* is conserved among all sequenced eukaryotic genomes. Amino acid sequence alignment reveals that the degree of identity between orthologous proteins is ~25% throughout the entire protein. We cloned a fragment of the human *NOP14* cDNA corresponding to amino acids 14–470 into pGAD and tested for interaction with pLexA-mEmg1 by two-hybrid assay. Measurements of β-galactosidase activity showed that the mammalian proteins interacted as strongly as their yeast orthologues, indicating that the association between Emg1 and Nop14 was also conserved (Liu and Thiele, unpublished results).

To confirm that yeast Emg1 and Nop14 physically interact in vivo, we coexpressed triple HA-Emg1 with double FLAG-Nop14 in yeast and performed coimmunoprecipitation. Both of these epitope-tagged proteins were capable of complementing the viability defect of the respective knockout

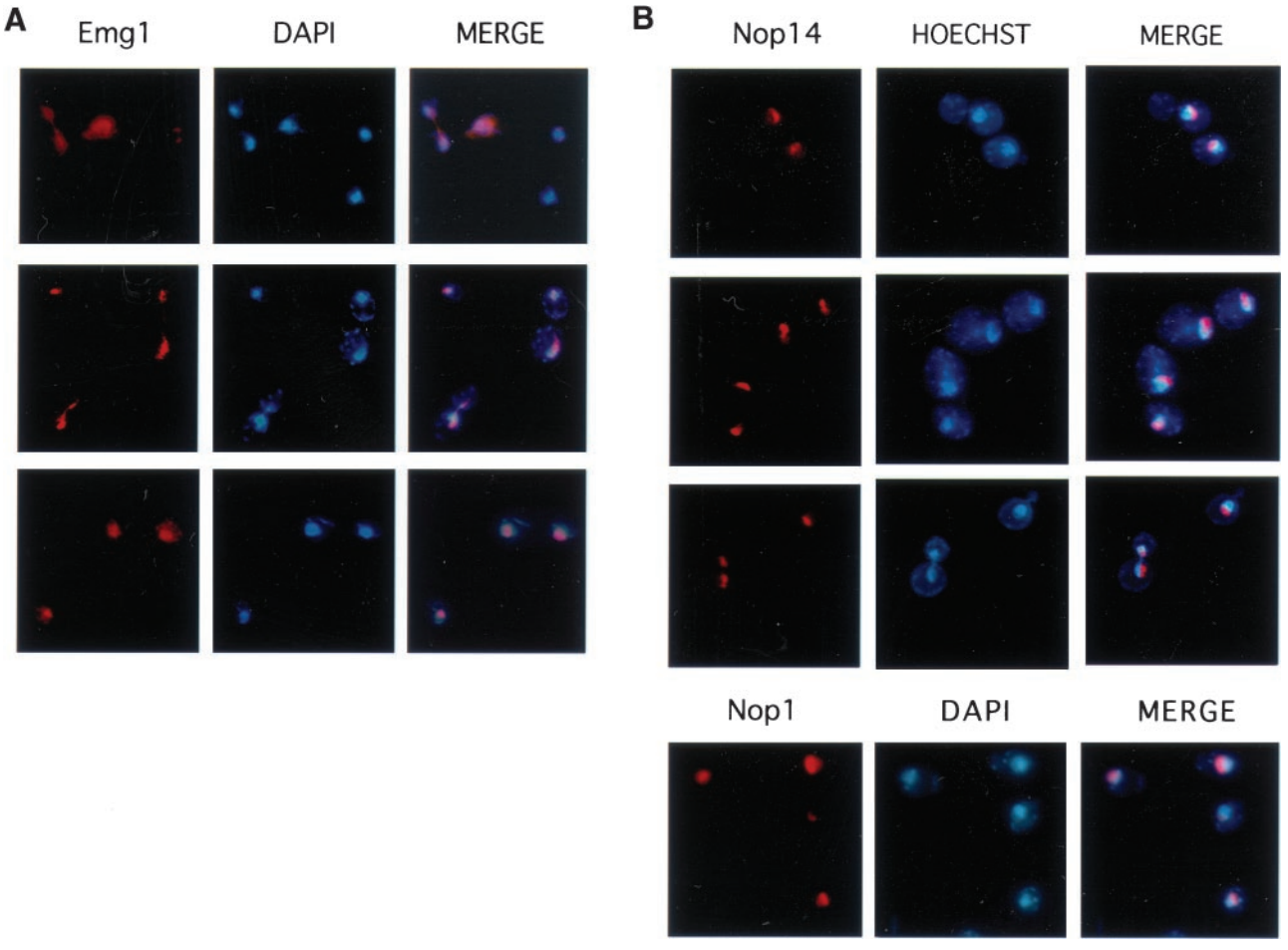

Figure 4. Localization of Emg1 to the nucleus and Nop14 to the nucleolus. (A) Indirect immunofluorescence photomicrographs of PLY12 (MYC-EMG1) cells stained with anti-MYC primary and goat anti-mouse-Texas Red secondary antibodies (red). Fixed cells were counterstained with DAPI to reveal the nuclear DNA. (B) Direct fluorescence images of PLY23 (NOP14-GFP) cells stained with Hoechst 33342. The crescent fluorescent signal that localizes adjacent to the nuclear signal is characteristic of the yeast nucleolus. (C) Indirect immunofluorescence with antibody specific to the nucleolar protein Nop1 reveals the same crescent pattern as seen for Nop14-GFP.

strains when expressed from centromeric plasmids (Liu and Thiele, unpublished results). As shown in Figure 2B, pull-down assays with anti-FLAG (M2) antibody followed by immunoblotting with anti-HA antibody revealed the presence of HA-Emg1 in the immunoprecipitates. HA-Emg1 was not detected in immunoprecipitates of control cells expressing only HA-Emg1 with wild-type Nop14 or only Nop14-FLAG with wild-type Emg1. Likewise, a reciprocal pull-down with the anti-HA antibody for Emg1 also specifically precipitated Nop14-FLAG. Although the interaction between these proteins appeared specific, the amount of each protein that was immunoprecipitated by the partner was not quantitative, suggesting that only a fraction of Emg1 and Nop14 were associated under our experimental conditions. In view of the broad distribution of Emg1, we wanted to localize Nop14 to ascertain where in yeast cells this interaction might occur. As shown in Figure 3C, Nop14-FLAG was detected predominantly in the nuclear fraction, like Nop1, suggesting that Nop14 might be a binding partner for the nuclear pool of Emg1.

Emg1 and Nop14 Localization by Fluorescence Microscopy

To verify the localization of Emg1 and Nop14 independently, we localized these proteins in yeast by fluorescence microscopy. We generated an MYC2-*EMG1* allele that fully complements the growth defects of the *emg1* knockout strain when expressed from a centromeric plasmid with the endogenous *EMG1* promoter (Figure 6). As shown in Figure 4A, the signal for MYC-Emg1 is focused in a single large spot that largely, but not completely, overlaps with the DAPI-stained chromatin with weaker staining in the cytoplasm. Indeed the nuclear fluorescence from MYC-Emg1 appears to extend beyond the boundaries of the chromatin, suggesting that Emg1 is also present in the nucleolus (e.g., Figure 4A, top). Overexpression of MYC-Emg1 from a multicopy plasmid or from the strong heterologous GPD promoter led to strong, even fluorescence throughout the cell, suggesting that the nuclear pool of Emg1 is saturable (Liu and Thiele, unpublished results). Fluorescence images of

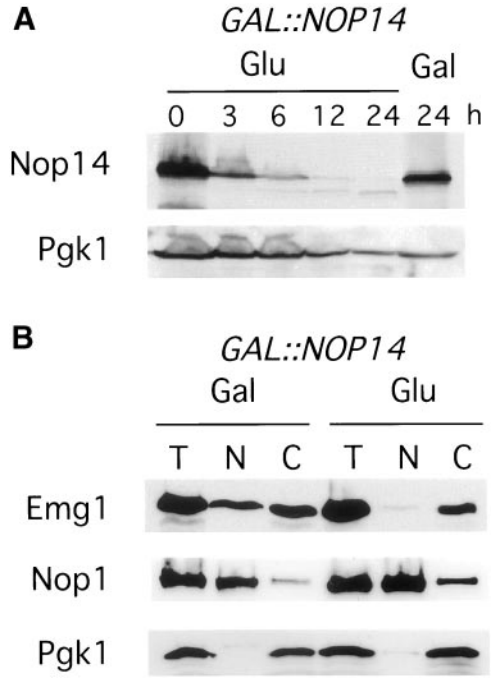

Figure 5. Nuclear localization of Emg1 requires Nop14. (A) Depletion of Nop14. PLY23 (GAL1-NOP14) cells were grown in YPGal medium until log phase and diluted into fresh YPGal (Gal) or YPD (Glu), and aliquots were harvested at the indicated times for analysis of Nop14-FLAG or Pgk1 levels by immunoblotting. (B) Emg1 is predominantly cytoplasmic in the absence of Nop14. Total cell (T), nuclear (N), and cytoplasmic (C) fractions were biochemically purified from PLY23 (GAL1-NOP14) cells cultured in YPGal (Gal) or shifted to YPD (Glu) for 9 h, and western blotting was performed with the use of anti-HA (for HA-EMG1), anti-Nop1, or anti-Pgk1 antibodies.

live cells expressing the Nop14-GFP fusion revealed a distinct crescent-shaped signal that is polarized to one side of the nucleus that is largely separate from the chromatin (Figure 4B). This pattern of localization is characteristic of yeast nucleolar antigens. Previously, Nop14 was found to copurify with nuclear pore complexes and was also reported to be a nuclear/nucleolar protein based on indirect immunofluorescence detection of a protein A-Nop14 fusion (Rout *et al.*, 2000); however, it was not reported in that study whether the protein A-Nop14 fusion was functional. To confirm the nucleolar localization of Nop14, we compared its localization to the well characterized nucleolar protein Nop1. Like Nop14, the signal for Nop1, detected by indirect immunofluorescence with the use of a monoclonal anti-NOP1 antibody, was localized to one side of the nucleus distinct from the nuclear DNA. Therefore, we conclude that Nop14 is primarily a nucleolar protein, whereas Emg1 is more widely distributed throughout the cell but with a clear nuclear signal.

Nuclear Localization of Emg1 Depends on Nop14

In view of the distribution of Emg1 to both cytoplasmic and nuclear compartments and its interaction with the nuclear protein Nop14, we asked whether localization of Emg1 to the nucleus requires the presence of Nop14. To test this hypothesis, we generated a yeast strain PLY23 (GAL1-NOP14) bearing the *NOP14*-FLAG allele under the control of the *GAL1* promoter. When these cells were shifted to glucose-containing media, the level of Nop14-FLAG was reduced to undetectable levels by 12 h (Figure 5A). The growth rate of these cells was indistinguishable from the wild-type parental strain over the first 16 h after shifting to glucose medium, and cessation of growth did not occur until after 30 h (Liu and Thiele, unpublished results). The distribution of Emg1 was ascertained in cells that were shifted to glucose medium for 10 h with the use of biochemical fractionation. In cells expressing Nop14, we detected HA-Emg1 in both the nuclear and cytoplasmic fractions, as expected; however, in cells depleted of Nop14, Emg1 was nearly absent from the nuclear fraction with little effect on either the total or cytoplasmic levels. To confirm that the effect was specific for Emg1, we also probed for the localization of Nop1. As shown, there was no effect on the nuclear distribution of Nop1. Likewise, the levels and cytoplasmic localization of Pgk1 were also unaffected. These data support the idea that the nuclear pool of Emg1 is either delivered or retained there through interactions with Nop14.

EMG1 Mutants Are Hypersensitive to Aminoglycoside Antibiotics

The nucleolus is the primary site for processing of rRNAs and tRNAs as well as assembly of several important ribonucleoprotein complexes including the ribosome (Pederson and Politz, 2000). The localization of Nop14 to the nucleolus prompted us to ask whether the interaction between Emg1 and Nop14 might have a potential role in RNA processing or ribosome biogenesis. To facilitate functional characterization of these proteins, we generated a conditional allele of *EMG1*. We isolated a temperature-sensitive allele of *EMG1*, *emg1-1*, that contains two point mutations (I104S, K109P) clustered within the highly conserved central region (Figure 1B). Cells bearing this allele, PLY12 (*MYC-emg1-1*), are impaired for growth above 37°C on rich medium (Figure 6A) even though levels of the mutant protein are not reduced at the elevated temperature (Liu and Thiele, unpublished results). A more severe phenotype with impaired growth above 25°C was observed in cells harboring an integrated MYC-*emg1-1* allele (Figure 5A, PLY21). The growth defect of PLY21 was completely reversed by episomal expression of *EMG1* (Liu and Thiele, unpublished results), indicating that this phenotype could be attributed to the mutations in the *emg1-1* allele.

Mutations in proteins involved in ribosome biogenesis or in RPs frequently exhibit altered sensitivity to drugs that affect protein translation. We compared the growth of *emg1-1* strains with an isogenic wild-type control using two classes of protein synthesis inhibitors, cycloheximide and the aminoglycosides paromomycin and neomycin. Whereas there was no altered sensitivity to cycloheximide, cells harboring the *emg1-1* allele were ~10-fold more sensitive to either neomycin or paromomycin at the permissive temperature of 25°C (Figure 6B). The effect was exacerbated at the semipermissive temperature of 34°C where the *emg1-1* strains were completely inhibited even by low concentrations of the drugs (Figure 6C).

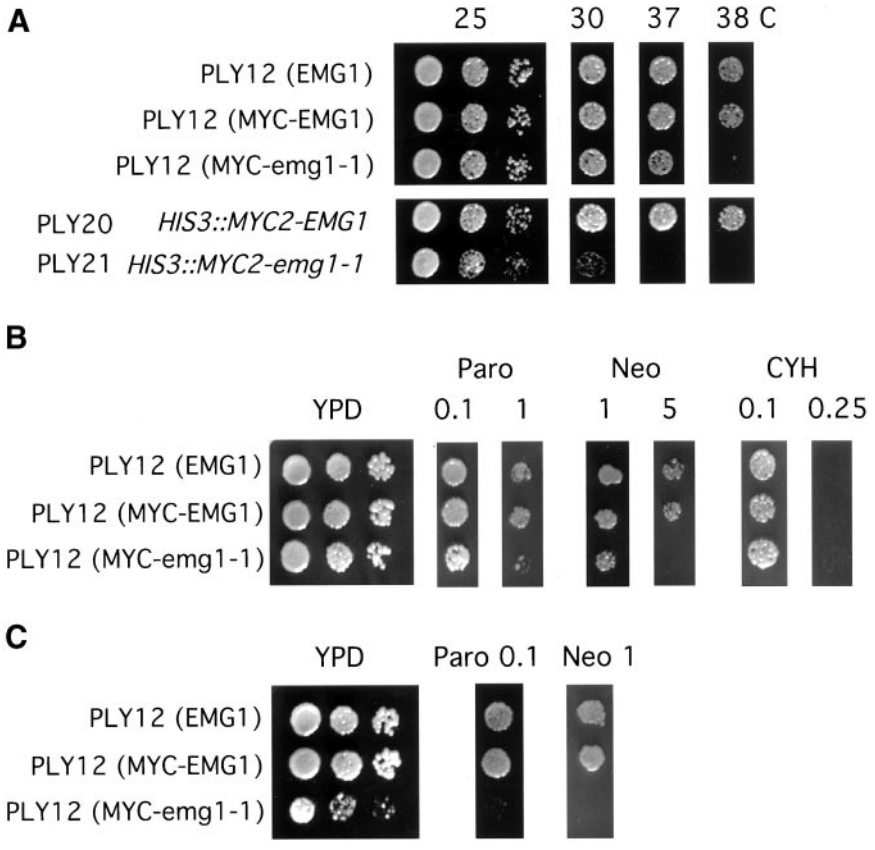

Figure 6. A conditional allele of *EMG1* is hypersensitive to aminoglycoside antibiotics. (A) *emg1* cells bearing CEN plasmids harboring wild-type *EMG1*, MYC2-*EMG1*, or MYC2-*emg1-1* or PLY20 or PLY21 with integrated alleles of MYC2-*EMG1* and MYC2-*emg1-1*, respectively, were grown to midlog phase and then serially diluted (OD_{600} 0.1, 0.01. 0.001, left to right) and spotted onto YPD plates. The plates were photographed after incubation for 2 d at the indicated temperatures. Only the middle dilution is shown for the 30, 37, and 38°C plates. (B) PLY12 harboring CEN plasmids for the indicated alleles of *EMG1* were grown to midlog phase, serially diluted, and spotted as in B onto plates containing various concentrations of the listed antibiotics. For paromomycin (Paro) and neomycin (Neo), the concentration is given in milligrams per milliliter and for cycloheximide (CYH) in micrograms per milliliter. (C) Sensitivity to paromomycin and neomycin is exacerbated in the *emg1-1* strain at the semipermissive temperature of 34°C.

Emg1 and Nop14 Are Required for 18S rRNA Processing

The data above show that mutations in *EMG1* sensitize cells to aminoglycoside antibiotics and suggest a potential role for Emg1 in the biogenesis or regulation of the small ribosomal subunit. To test this hypothesis directly, we analyzed the processing of the rRNA transcript in vivo by pulse-chase labeling with [*methyl*-^{3}H]methionine, the methyl donor for incorporation into rRNA by methylases during posttranscriptional processing. PLY21 cells or isogenic wild-type controls were cultured overnight in YPD at 23°C to log phase and then diluted into YPD prewarmed to 37°C and cultured for 10 h at the restrictive temperature before pulse-chase labeling. As shown in Figure 7A, wild-type cells quickly processed the primary 35S rRNA transcript into the 20S and 27S intermediates (time 0) and then generated the mature 18S and 25S species. In contrast, a delay in processing was observed in PLY21 cells, even those maintained at the permissive temperature of 23°C, as evidenced by the increased levels of the 35S precursor. Significantly, there was a reduction in the level of mature 18S RNA as judged by the ratio of 25S to 18S compared with wild-type cells. This defect appeared to be primarily at the level of 20S maturation because the small amount of 20S present in *emg1-1* strains at the 2-min time point was still processed to the 18S at the permissive temperature. This effect was exacerbated in cells shifted to the nonpermissive temperature: at 37°C, processing to 18S RNA is further reduced and virtually no mature 18S or the 20S precursor RNA is detectable. Although there was a kinetic delay in the formation of the 25S rRNA in the *emg1-1* strain, the levels were not diminished compared with wild-type cells, indicating that cells harboring the *emg1-1* mutation were selectively impaired for processing of the 18S rRNA, consistent with the selective sensitivity to aminoglycoside drugs.

In a parallel experiment, rRNA processing was followed in cells depleted of Nop14 (PLY23 [GAL-NOP14]). We subjected these cells to an identical pulse-chase experiment 8 h after repressing *GAL::NOP14* expression (Figure 7B). Cells depleted of Nop14 showed a similar defect in 18S processing as cells harboring the *emg1-1* mutation at the restrictive temperature. Whereas processing of the 25S rRNA appeared normal, there was a conspicuous absence of the 18S rRNA species and its 20S precursor. The similarity in phenotype between the *Nop14* and *emg1* mutants supports the idea that these proteins act in the same pathway for the production of the mature 18S rRNA.

To extend this analysis, we performed RNA blotting with the use of oligonucleotides specific for distinct regions of the primary rRNA transcript to measure steady-state levels of the processing intermediates (Figure 8A). A gross analysis of the 18S levels with the use of ethidium bromide staining (Liu and Thiele, unpublished results) or hybridization to an 18S-specific probe in cells (PLY23 [GAL-NOP14]) depleted of NOP14 by shift to glucose revealed a decrease in steady-state levels of this RNA in concordance with the defect in

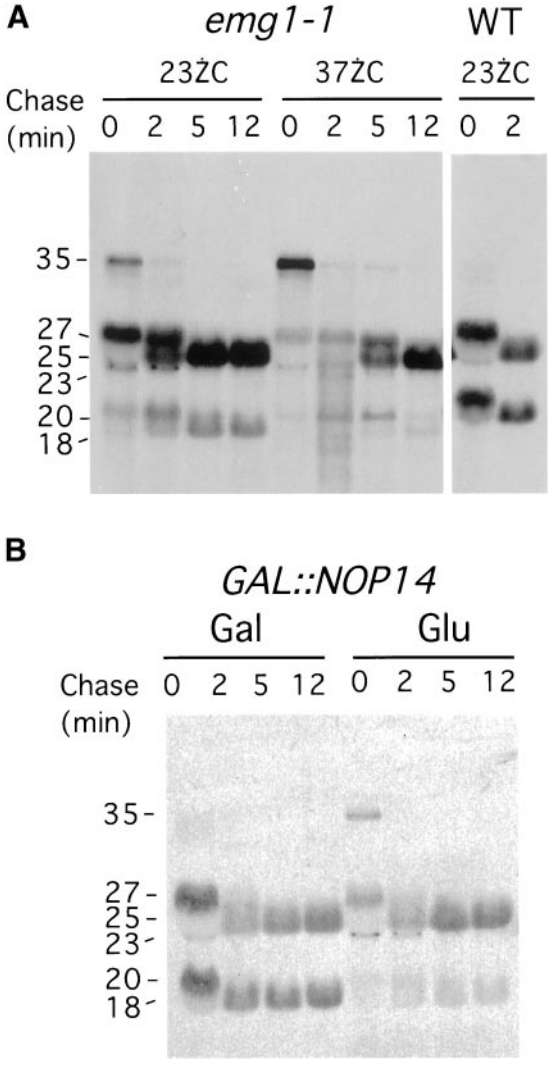

Figure 7. Maturation of the 18S rRNA requires Emg1 and Nop14. (A) PLY21 (*emg1:: LEU2 HIS3::emg1-1*) cells were grown at the permissive temperature (23°C), subcultured into SCD-met, and either maintained at 23° or shifted to 37°C for 9 h. The isogenic W303–1α strain (wild type, WT) was similarly shifted to 37°C. Cells were pulse labeled with [*methyl*-^{3}H]methionine as described, and pre- and mature rRNA species (indicated by hash marks) were detected by fluorography. In the wild-type strain, rRNA processing was completed by 2 min of chase. (B) PLY23 (GAL1-NOP14) cells were grown in YPGal medium until log phase and subcultured into either SCGAL-met (control) or SCD-met (ENP shutoff) and incubated for 8 h. The RNA was labeled and processed as in A.

18S maturation (Figure 8B, probe b). In addition, there is a clear diminution of the 20S pre-rRNA, the precursor to the 18S rRNA in the Nop14-depleted cells (Figure 8B, probe c) beginning as early as 6 h after glucose shutoff. The levels of 20S were further decreased at 12 and 24 h, times at which Nop14 is virtually undetectable by immunoblotting (Figure 5A). Simultaneously there was accumulation of the 35S precursor rRNA transcript in cells depleted of Nop14 (Figure 8B, see probes a, c, and d) and the appearance of another intermediate, the 23S pre-rRNA. The 23S product has been previously characterized as an aberrant species formed from cleavage at site A_3 without prior processing at sites A_0-A_2 (Venema and Tollervey, 1999). In agreement with the pulse-chase analysis of rRNA processing, there appears to be no defect in the maturation of the 25S rRNA (Figure 8B, probe e). To examine processing in yeast harboring the *emg1-1* allele, we compared strain PLY21 to its isogenic wild-type control PLY20. The rRNA-processing defect in *emg1-1* cells at the semipermissive temperature of 34°C was virtually indistinguishable from the phenotype of *nop14* cells. Specifically, there was an accumulation of the 35S precursor and reduced levels of mature 18S rRNA and the 20S precursor with no defect in steady-state levels of the 25S rRNA (data not shown). Collectively, the RNA blot and pulse-chase analyses demonstrate that Emg1 and Nop14 are required in the pathway leading to18S rRNA maturation but are dispensable for 25S rRNA processing.

Emg1 and Nop14 Are Required for 40S Ribosome Biogenesis

Because mutations in *EMG1* or depletion of Nop14 lead to decreased production of 18S rRNA, the RNA component of the 40S ribosome, we reasoned that cellular levels of the small ribosomal subunit would be diminished in these cells. To test this hypothesis, we profiled cellular ribosomes by sucrose density gradients. As shown in Figure 9A, isogenic wild-type (W303–1a) and PLY23 (GAL-NOP14) cells grown in galactose had a typical polysome profile consisting of the 40S and 60S subunits, the 80S monoribosome, and seven to eight polysomes (Figure 9A). In contrast, PLY23 cells depleted of Nop14 by growth in glucose for 10 h had a significantly reduced 40S peak and a dramatically enlarged 60S peak consistent with a defect in 18S processing and accumulation of free large ribosomal subunits. Likewise, this subunit imbalance was observed in PLY21 strains bearing the *emg1-1* allele. Even at the permissive growth temperature of 23°C, there was a relative decrease in levels of the 40S subunit and accumulation of free 60S subunits compared with the isogenic control strain PLY20 (Figure 9B). This effect in the PLY21 strain was specifically attributable to the point mutations in the *EMG1* ORF and not to the MYC epitope because a strain bearing a nontagged allele of *emg1-1* also resulted in a qualitatively similar subunit imbalance (Liu and Thiele, unpublished results). On shift to the restrictive temperature, there was a further diminution of the 40S peak as well as an overall decrease in polysomes. To quantify the deficiency of 40S subunits in these mutant strains, we measured cellular levels of 40S and 60S subunits by allowing polysome runoff from transcripts and prepared extracts under ribosome-dissociating conditions. Analysis of sucrose gradients prepared without Mg^{2+} revealed a large increase in the 60S to 40S subunit ratio in PLY21 cells compared with wild-type cells (Figure 9C). The inset shows that the ratio of 60S subunits to 40S was increased more than threefold in both the *emg1-1* strain and in cells depleted of Nop14 when compared with isogenic wild-type strains, thus confirming the defect in 40S biogenesis.

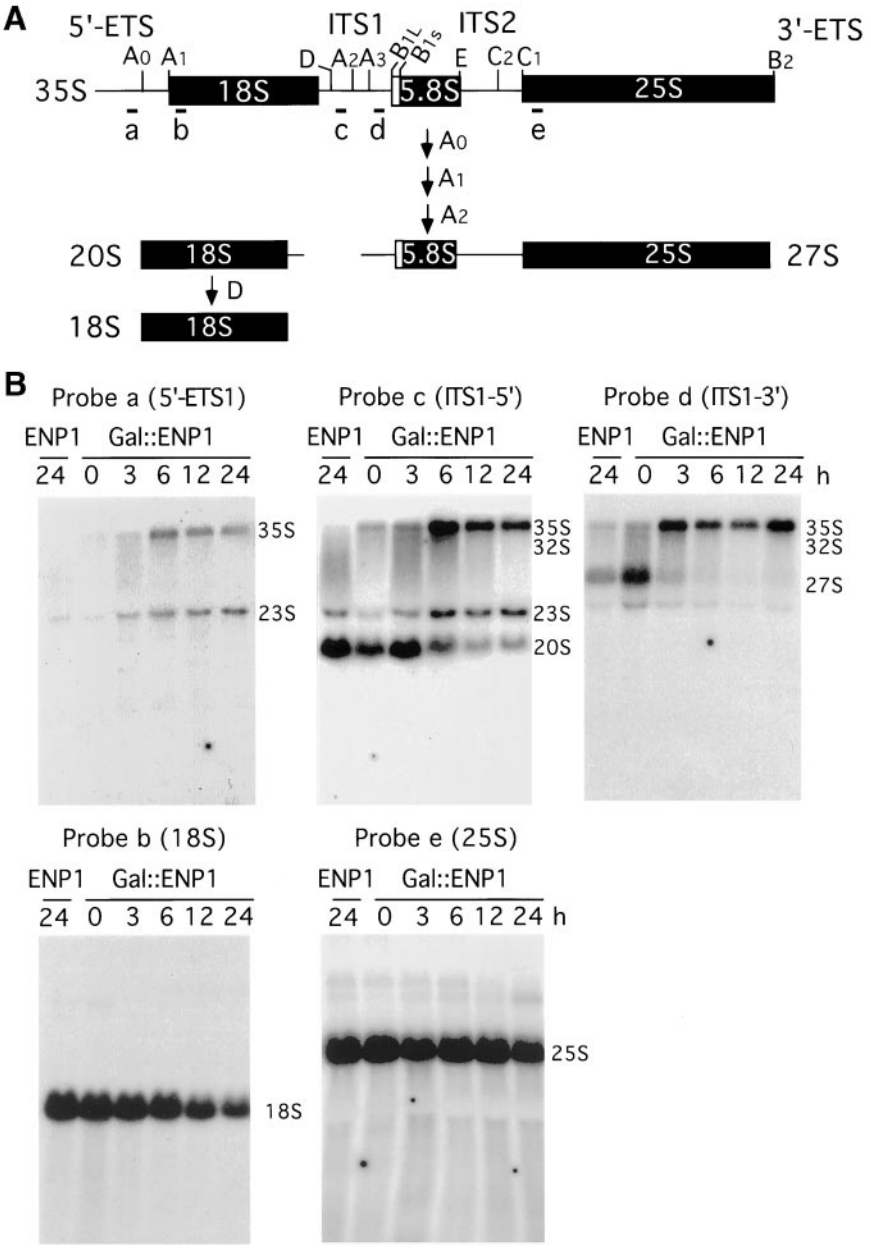

Figure 8. Processing defects in the 35S pre-rRNA transcript in *EMG1* or *NOP14* mutants. (A) Schematic of the 35S pre-RNA and the major processing sites in *S. cerevisiae*. The 35S pre-rRNA primary transcript encodes the 18S, 5.8S, and 25S rRNA sequences separated by two internal transcribed spacers (ITS1 and ITS2). Two external transcribed spacers (5′-ETS and 3′-ETS) flank each end of the transcript. The letters with subscripts denote the ordered cleavage sites. Small bars identified by lowercase letters indicate positions of the oligonucleotide probes. (B) Steady-state levels of pre- and mature rRNA species in PLY23 (*Nop14:: KAN^R*, *GAL1:: NOP14*) and *NOP14* control (PLY23, p413*NOP14*) cells that were grown in YPGal and shifted to YPD for the indicated times. The oligonucleotide probes used in the experiment are indicated above each autoradiograph. The position of each rRNA species is indicated.

DISCUSSION

In this study, we have identified the previously uncharacterized proteins Emg1 and an interacting protein Nop14 as essential for maturation of the18S rRNA and 40S ribosome biogenesis. Initially, we identified *EMG1* as a stress-responsive mRNA with a gene expression pattern that was similar to numerous genes encoding proteins involved in ribosome production. The *EMG1* and *NOP14* mRNAs are strongly reduced in response to heat shock and other environmental stress conditions with a magnitude and kinetics of response similar to RP genes (Figure 1A). Cluster analysis of genes coregulated with *EMG1* or *NOP14* with the use of a large data set for the response of the yeast genome to numerous environmental stresses reveals that *EMG1* and *NOP14* are members of the repressed environmental stress response (ESR) genes, which includes genes encoding RPs and other proteins involved in RNA metabolism and protein synthesis (Gasch *et al.*, 2000). Virtually all RP genes are transcriptionally coregulated by the abundant DNA-binding proteins Rap1 or Abf1 (Lascaris *et al.*, 1999; Warner, 1999); however, among non-RP genes of the ESR, two additional, conserved regulatory motifs, designated RRPE (rRNA-processing element) and the PAC box, have been identified by sequence alignment (Hughes *et al.*, 2000). Inspection of the *EMG1* promoter sequence reveals the presence of both an RRPE and PAC box as well as tandem repeats of the Abf1 site.

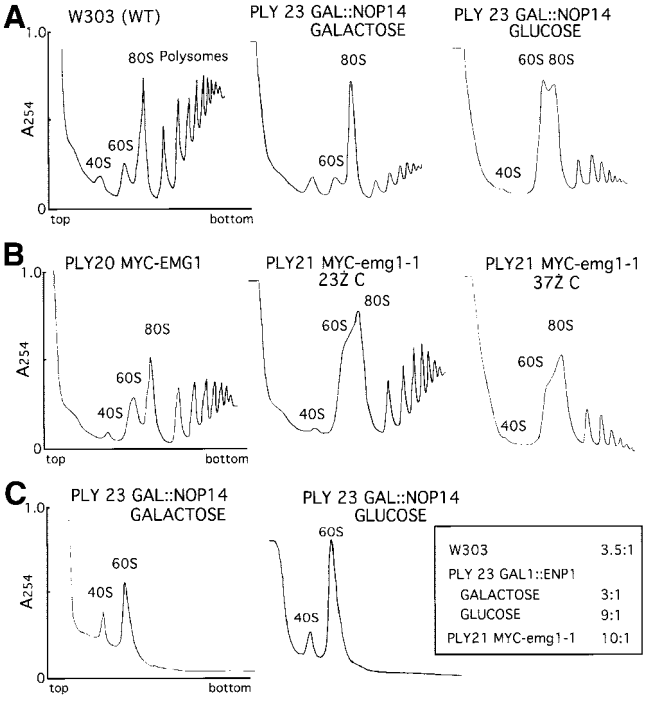

Figure 9. Yeast depleted of Nop14 or harboring *emg1-1* have diminished levels of 40S ribosomal subunits. (A) Polysome analysis of PLY23 (GAL1-NOP14) cells grown in YPGal medium or depleted of Nop14 by shifting to YPD for 12 h. Parental wild-type (WT) strain W303–1a is shown as a control. The 40S and 60S ribosomal subunits and the 80S ribosome and polysomes are indicated. (B) Polysome analysis of PLY21 cells grown at 23° or shifted to 37°C for 12 h. Polysome profile of identically treated PLY20 cells shifted to 37°C for 12 h is shown for comparison. (C) Decreased 40S to 60S ratio in cells depleted of Nop14. Polysome profiles were analyzed under ribosome dissociating conditions to reveal cellular amounts of the 40S and 60S ribosome subunits. The inset shows the ratio of 60S to 40S in each strain.

Similarly, the *NOP14* promoter, like numerous other ESR genes, also possesses these three elements (Gasch *et al.*, 2000; Causton *et al.*, 2001).

Although transcript profiling of *EMG1* and *NOP14* only suggested a putative link to ribosome production or function, our genetic and biochemical data strongly support a specific role for Emg1 and Nop14 in the biogenesis of the small ribosomal subunit. First, cells harboring a temperature-sensitive allele of *EMG1* showed a depletion of 40S subunits and a corresponding accumulation of free 60S subunits at the restrictive temperature. We note that even at the permissive temperature the *emg1-1* strain was defective for 40S ribosome subunits even though it showed little difference in growth rates compared with the wild-type strain. Consistent with the cellular deficit of 40S particles, analysis of rRNA processing by either pulse-chase labeling with [*methyl*-^{3}H]methionine or RNA blot analysis demonstrated a severe decrease in the efficiency of 18S rRNA processing leading to a gradual diminution of steady-state levels of 18S rRNA in the mutant strains. These experiments revealed that the major defect was diminished generation of the 20S pre-rRNA with concomitant production of an aberrant 23S species (Venema and Tollervey, 1995). This pattern of processing has also been observed in yeast harboring conditional alleles in genes required for 40S biogenesis, including several RNA helicases (Rok1, Rrp3, Fal1; Venema and Tollervey, 1995; O'Day *et al.*, 1996; Kressler *et al.*, 1997), nucleolar proteins (Nop1, Gar1, Sof1, Nop5; Tollervey *et al.*, 1991; Girard *et al.*, 1992; Jansen *et al.*, 1993; Wu *et al.*, 1998), and several snoRNAs (U3, U14, snR30; Li *et al.*, 1990; Hughes and Ares, 1991; Morrissey and Tollervey, 1993) as well as the RNA methylase Dim1 (Lafontaine *et al.*, 1995). These snoRNAs and nucleolar proteins are thought to make up a large snoRNP complex that is important for the early A_0, A_1, and A_2 cleavages (Kressler *et al.*, 1999). Mutations blocking these early processing steps without affecting the later A_3 cleavage lead to the generation of the dead-end 23S species and the 27S pre-rRNA (Venema and Tollervey, 1995). The latter can be processed into the mature 5.8S and 25S rRNAs; therefore, no decrease in 25S rRNA or in the 60S ribosomal subunit was observed in *emg1-1* cells. Importantly, cells depleted of Nop14 also exhibited a nearly identical phenotype, implicating these proteins in the same biochemical pathway. These data also support the idea the physical interaction between Emg1 and Nop14 in vivo is functionally relevant. Finally, cells harboring the *emg1-1* allele show enhanced sensitivity to the aminoglycoside antibiotics neomycin and paromomycin. Sensitivity to aminoglycoside drugs has been previously demonstrated in *fal1-1* and *nsr1* cells, which also manifest a 40S defect (Lee *et al.*, 1992; Kressler *et al.*, 1997), consistent with structural data showing direct binding of these compounds to the small ribosomal subunit (Carter *et al.*, 2000). Together, these observations support a model in which Emg1 and Nop14 are involved in the early cleavage or methylation events of the 35S pre-rRNA and are required for 40S ribosome biogenesis.

The predominant nucleolar localization of Nop14 is consistent with its proposed role in the rRNA processing. Inspection of the Nop14 amino acid sequence does not reveal any characteristic nucleolar protein motifs, such as GAR boxes, acidic/Ser-rich regions, or RNA recognition motifs. *NOP14* does contain several KKX motifs as observed in Nop5 and Nop56 (Gautier *et al.*, 1997; Wu *et al.*, 1998); however, these sequences are scattered throughout the Nop14 protein rather than concentrated within a defined motif. In contrast, Emg1 is widely distributed within the cell as determined by biochemical and cytological analyses. The steady-state nuclear localization of Emg1, however, depends on the presence of Nop14. Depletion of Nop14 results in a significant depletion of nuclear Emg1, suggesting that the interaction between Nop14 and Emg1 is required for Emg1 residence in the nucleus/nucleolus. One possibility for this broad distribution might be that Emg1 plays multiple roles in the maturation of the 18S rRNA and 40S biogenesis. The Nip7 protein, required for 60S ribosome biogenesis, also has a similar broad distribution and associates with the large ribosomal subunit in the cytoplasm, suggesting a potential role in cytosolic 60S maturation in addition to a role in rRNA processing (Zanchin and Goldfarb, 1999). Immunoblot analysis of Emg1 distribution in sucrose density gradients, however, revealed that Emg1 does not cofractionate with the 40S peak, suggesting that cytosolic Emg1 does not associate with the ribosomal subunit (Liu and Thiele, unpublished results). Several nucleolar proteins including nucleolin, the mamma-

lian homologue of yeast Nsr1, undergo nucleocytoplasmic shuttling, but the functional significance of this trafficking remains largely unknown (Kondo and Inouye, 1992; Lee *et al.*, 1992; Ginisty *et al.*, 1998, 1999). Recently a unique function for the nucleolar protein Rrb1 was reported in regulating 60S ribosome biogenesis through direct physical interactions with RPL3 and regulation of *RPL3* gene expression. A remarkable observation was the coupling of Rrb1 nuclear localization with ongoing protein translation, suggesting that the shuttling of the proposed Rrb1-rpL3 complex might be coordinated with the active requirement for RPs in ribosome biogenesis (Iouk *et al.*, 2001). Potentially, Emg1 could play an analogous role as Rrb1 for a 40S-specific factor by facilitating the movement of this factor from the cytoplasm to the nucleolus where interactions between Emg1 and Nop14 would allow assembly of its potential cargo into the pre-rRNA RNP.

A previous study of the fission yeast orthologue of Emg1, called Mra1, suggested that Mra1 might genetically interact with the Ras-signaling pathway, because overexpression of *mra1* suppressed an allelic *ras1* mutation that resulted in inefficient mating (Hakuno *et al.*, 1996). Epistasis experiments, however, indicated that Mra1 suppression of the *rasS40T* allele was indirect. Interestingly, several alleles of *mraI* were isolated in which the ability to suppress the mating defect was separate from its essential cellular requirement, suggesting that Mra1 may be involved in multiple cellular pathways. Our analysis of the baker's yeast Emg1 clearly supports the idea that Emg1 is required for correct processing of the rRNA precursor to the18S rRNA. In view of the high degree of structural conservation in the Emg1 protein and lack of other similar sequences in eukaryotic genomes, we predict that the essential requirement for Emg1 in yeast and other eukaryotes is related to this function. Together with the nucleolar protein Nop14, these members of the repressed ESR gene cluster constitute new components of the 40S ribosome biogenesis machinery.

ACKNOWLEDGMENTS

We thank Kevin Morano, David Engelke, and Janine Maddock for advice, discussions, and critical readings of this work. We thank Ursula Jacob, Hans Bugel, Jennifer Fuentes, Kaustuv Datta, and Bin Lin for advice and assistance with ribosome profiling and analysis. We appreciate the fine technical assistance from Chen Kuang. We thank John Aris, Kathryn Tullis, Philip James, and Elizabeth Craig for gifts of reagents. This work was supported by National Research Service Award postdoctoral fellowship GM-18858 (to P.C.C.L.) and grant GM-59911 (to D.J.T.) from the National Institutes of Health.

REFERENCES

Ansari-Lari, M.A., Oeltjen, J.C., Schwartz, S., Zhang, Z., Muzny, D.M., Lu, J., Gorrell, J.H., Chinault, A.C., Belmont, J.W., Miller, W., and **Gibbs, R.A.** (1998). Comparative sequence analysis of a gene-rich cluster at human chromosome 12p13 and its syntenic region in mouse chromosome 6. Genome Res. *8*, 29–40.

Aris, J.P., and Blobel, G. (1988). Identification and characterization of a yeast nucleolar protein that is similar to a rat liver nucleolar protein. J. Cell Biol. *107*, 17–31.

Baim, S.B., Pietras, D.F., Eustice, D.C., and Sherman, F. (1985). A mutation allowing an mRNA secondary structure diminishes translation of *Saccharomyces cerevisiae* iso-1-cytochrome c. Mol. Cell. Biol *5*, 1839–1846.

Boeke, J.D., Trueheart, J., Natsoulis, G., and Fink, G.R. (1987). 5-Fluoroorotic acid as a selective agent in yeast molecular genetics. Methods Enzymol. *154*, 164–175.

Carter, A.P., Clemons, W.M., Brodersen, D.E., Morgan-Warren, R.J., Wimberly, B.T., and Ramakrishnan, V. (2000). Functional insights from the structure of the 30S ribosomal subunit and its interactions with antibiotics. Nature *407*, 340–348.

Causton, H.C., Ren, B., Koh, S.S., Harbison, C.T., Kanin, E., Jennings, E.G., Lee, T.I., True, H.L., Lander, E.S., and Young, R.A. (2001). Remodeling of yeast genome expression in response to environmental changes. Mol. Biol. Cell *12*, 323–337.

Chu, S., DeRisi, J., Eisen, M., Mulholland, J., Botstein, D., Brown, P.O., and Herskowitz, I. (1998). The transcriptional program of sporulation in budding yeast. Science *282*, 699–705.

DeRisi, J.L., Iyer, V.R., and Brown, P.O. (1997). Exploring the metabolic and genetic control of gene expression on a genomic scale. Science *278*, 680–686.

Eisen, M.B., Spellman, P.T., Brown, P.O., and Botstein, D. (1998). Cluster analysis and display of genome-wide expression patterns. Proc. Natl. Acad. Sci. USA *95*, 14863–14868.

Franzusoff, A., Rothblatt, J., and Schekman, R. (1991). Analysis of polypeptide transit through yeast secretory pathway. Methods Enzymol. *194*, 662–674.

Gasch, A.P., Spellman, P.T., Kao, C.M., Carmel-Harel, O., Eisen, M.B., Storz, G., Botstein, D., and Brown, P.O. (2000). Genomic expression programs in the response of yeast cells to environmental changes. Mol. Biol. Cell *11*, 4241–4257.

Gautier, T., Berges, T., Tollervey, D., and Hurt, E. (1997). Nucleolar KKE/D repeat proteins Nop56p and Nop58p interact with Nop1p and are required for ribosome biogenesis. Mol. Cell. Biol *17*, 7088–7098.

Gietz, D., St. Jean, A., Woods, R.A., and Schiestl, R.H. (1992). Improved method for high efficiency transformation of intact yeast cells. Nucleic Acids Res. *20*, 1425.

Ginisty, H., Amalric, F., and Bouvet, P. (1998). Nucleolin functions in the first step of ribosomal RNA processing. EMBO J. *17*, 1476–1486.

Ginisty, H., Sicard, H., Roger, B., and Bouvet, P. (1999). Structure and functions of nucleolin. J. Cell Sci. *112*, 761–772.

Girard, J.P., Lehtonen, H., Caizergues-Ferrer, M., Amalric, F., Tollervey, D., and Lapeyre, B. (1992). GAR1 is an essential small nucleolar RNP protein required for pre-rRNA processing in yeast. EMBO J. *11*, 673–682.

Gorenstein, C., and Warner, J.R. (1976). Coordinate regulation of the synthesis of eukaryotic ribosomal proteins. Proc. Natl. Acad. Sci. USA *73*, 1547–1551.

Hadano, S., Ishida, Y., and Ikeda, J.E. (1998). The primary structure and genomic organization of five novel transcripts located close to the Huntington's disease gene on human chromosome 4p16.3. DNA Res. *5*, 177–186.

Hakuno, F., Hughes, D.A., and Yamamoto, M. (1996). The *Schizosaccharomyces pombe* mra1 gene, which is required for cell growth and mating, can suppress the mating inefficiency caused by a deficit in the Ras1 activity. Genes Cells *1*, 303–315.

Herruer, M.H., Mager, W.H., Raue, H.A., Vreken, P., Wilms, E., and Planta, R.J. (1988). Mild temperature shock affects transcription of yeast ribosomal protein genes as well as the stability of their mRNAs. Nucleic Acids Res. *16*, 7917–7929.

Holstege, F.C., Jennings, E.G., Wyrick, J.J., Lee, T.I., Hengartner, C.J., Green, M.R., Golub, T.R., Lander, E.S., and Young, R.A. (1998). Dissecting the regulatory circuitry of a eukaryotic genome. Cell *95*, 717–728.

Hughes, J.D., Estep, P.W., Tavazoie, S., and Church, G.M. (2000). Computational identification of cis-regulatory elements associated with groups of functionally related genes in *Saccharomyces cerevisiae*. J. Mol. Biol. *296*, 1205–1214.

Hughes, J.M., and Ares, M., Jr. (1991). Depletion of U3 small nucleolar RNA inhibits cleavage in the 5′ external transcribed spacer of yeast pre-ribosomal RNA and impairs formation of 18S ribosomal RNA. EMBO J. *10*, 4231–4239.

Iouk, T.L., Aitchison, J.D., Maguire, S., and Wozniak, R.W. (2001). Rrb1p, a yeast nuclear WD-repeat protein involved in the regulation of ribosome biosynthesis. Mol. Cell. Biol. *21*, 1260–1271.

Jansen, R., Tollervey, D., and Hurt, E.C. (1993). A U3 snoRNP protein with homology to splicing factor PRP4 and G beta domains is required for ribosomal RNA processing. EMBO J. *12*, 2549–2558.

Kim, C.H., and Warner, J.R. (1983). Mild temperature shock alters the transcription of a discrete class of *Saccharomyces cerevisiae* genes. Mol. Cell. Biol. *3*, 457–465.

Kondo, K., and Inouye, M. (1992). Yeast NSR1 protein that has structural similarity to mammalian nucleolin is involved in pre-rRNA processing. J. Biol. Chem. *267*, 16252–16258.

Kressler, D., de la Cruz, J., Rojo, M., and Linder, P. (1997). Fal1p is an essential DEAD-box protein involved in 40S-ribosomal-subunit biogenesis in *Saccharomyces cerevisiae*. Mol. Cell. Biol. *17*, 7283–7294.

Kressler, D., Linder, P., and de La Cruz, J. (1999). Protein transacting factors involved in ribosome biogenesis in *Saccharomyces cerevisiae*. Mol. Cell. Biol. *19*, 7897–7912.

Lafontaine, D., Vandenhaute, J., and Tollervey, D. (1995). The 18S rRNA dimethylase Dim1p is required for pre-ribosomal RNA processing in yeast. Genes Dev. *9*, 2470–2481.

Lascaris, R.F., Mager, W.H., and Planta, R.J. (1999). DNA-binding requirements of the yeast protein Rap1p as selected in silico from ribosomal protein gene promoter sequences. Bioinformatics *15*, 267–277.

Lee, W.C., Zabetakis, D., and Melese, T. (1992). NSR1 is required for pre-rRNA processing and for the proper maintenance of steady-state levels of ribosomal subunits. Mol. Cell. Biol. *12*, 3865–3871.

Li, H.D., Zagorski, J., and Fournier, M.J. (1990). Depletion of U14 small nuclear RNA (snR128) disrupts production of 18S rRNA in *Saccharomyces cerevisiae*. Mol. Cell. Biol. *10*, 1145–1152.

Li, Y., Moir, R.D., Sethy-Coraci, I.K., Warner, J.R., and Willis, I.M. (2000). Repression of ribosome and tRNA synthesis in secretion-defective cells is signaled by a novel branch of the cell integrity pathway. Mol. Cell. Biol. *20*, 3843–3851.

Liu, X.D., Liu, P.C.C., Santoro, N., and Thiele, D.J. (1997). Conservation of a stress response: human heat shock transcription factors functionally substitute for yeast HSF. EMBO J. *16*, 6466–6477.

Lopez, N., Halladay, J., Walter, W., and Craig, E.A. (1999). SSB, encoding a ribosome-associated chaperone, is coordinately regulated with ribosomal protein genes. J. Bacteriol. *181*, 3136–3143.

Mager, W.H., and Planta, R.J. (1990). Multifunctional DNA-binding proteins mediate concerted transcription activation of yeast ribosomal protein genes. Biochim. Biophys. Acta *1050*, 351–355.

Morrissey, J.P., and Tollervey, D. (1993). Yeast snR30 is a small nucleolar RNA required for 18S rRNA synthesis. Mol. Cell. Biol. *13*, 2469–2477.

O'Day, C.L., Chavanikamannil, F., and Abelson, J. (1996). 18S rRNA processing requires the RNA helicase-like protein Rrp3. Nucleic Acids Res. *24*, 3201–3207.

Pederson, T., and Politz, J.C. (2000). The nucleolus and the four ribonucleoproteins of translation. J. Cell Biol. *148*, 1091–1095.

Planta, R.J. (1997). Regulation of ribosome synthesis in yeast. Yeast *13*, 1505–1518.

Ross-Macdonald, P., Coelho, P.S., Roemer, T., Agarwal, S., Kumar, A., Jansen, R., Cheung, K.H., Sheehan, A., Symoniatis, D., Umansky, L., Heidtman, M., Nelson, F.K., Iwasaki, H., Hager, K., Gerstein, M., Miller, P., Roeder, G.S., and Snyder, M. (1999). Large-scale analysis of the yeast genome by transposon tagging and gene disruption. Nature *402*, 413–418.

Rout, M.P., Aitchison, J.D., Suprapto, A., Hjertaas, K., Zhao, Y., and Chait, B.T. (2000). The yeast nuclear pore complex: composition, architecture, and transport mechanism. J. Cell Biol. *148*, 635–651.

Scheer, U., and Hock, R. (1999). Structure and function of the nucleolus. Curr. Opin. Cell Biol. *11*, 385–390.

Tollervey, D., Lehtonen, H., Carmo-Fonseca, M., and Hurt, E.C. (1991). The small nucleolar RNP protein NOP1 (fibrillarin) is required for pre- rRNA processing in yeast. EMBO J. *10*, 573–583.

Venema, J., and Tollervey, D. (1995). Processing of pre-ribosomal RNA in *Saccharomyces cerevisiae*. Yeast *11*, 1629–1650.

Venema, J., and Tollervey, D. (1999). Ribosome synthesis in *Saccharomyces cerevisiae*. Annu. Rev. Genet. *33*, 261–311.

Vojtek, A.B., Hollenberg, S.M., and Cooper, J.A. (1993). Mammalian Ras interacts directly with the serine/threonine kinase Raf. Cell *74*, 205–214.

Wach, A., Brachat, A., Pohlmann, R., and Philippsen, P. (1994). New heterologous modules for classical or PCR-based gene disruptions in *Saccharomyces cerevisiae*. Yeast *10*, 1793–1808.

Warner, J.R. (1999). The economics of ribosome biosynthesis in yeast. Trends Biochem. Sci. *24*, 437–440.

Wise, J.A. (1991). Preparation and analysis of low molecular weight RNAs and small ribonucleoproteins. Methods Enzymol. *194*, 405–415.

Wu, P., Brockenbrough, J.S., Metcalfe, A.C., Chen, S., and Aris, J.P. (1998). Nop5p is a small nucleolar ribonucleoprotein component required for pre-18 S rRNA processing in yeast. J. Biol. Chem. *273*, 16453–16463.

Zanchin, N.I., and Goldfarb, D.S. (1999). Nip7p interacts with Nop8p, an essential nucleolar protein required for 60S ribosome biogenesis, and the exosome subunit Rrp43p. Mol. Cell. Biol. *19*, 1518–1525.